A Monte Carlo investigation of plasmonic noise in nanometric n-$In_{0.53}Ga_{0.47}As$ channels

2009 J. Stat. Mech. 2009 P01040

(http://iopscience.iop.org/1742-5468/2009/01/P01040)

Journal of Statistical Mechanics: Theory and Experiment
An IOP and SISSA journal

A Monte Carlo investigation of plasmonic noise in nanometric n-$In_{0.53}Ga_{0.47}As$ channels

J-F Millithaler[1], L Reggiani[1], J Pousset[2], L Varani[2], C Palermo[2], W Knap[3], J Mateos[4], T González[4], S Perez[4] and D Pardo[4]

[1] Dipartimento di Ingegneria dell'Innovazione and CNISM, Università del Salento, Via Arnesano s/n, 73100 Lecce, Italy
[2] Institut d'Électronique du Sud, UMR CNRS 5214, Université Montpellier II, place Bataillon, 34095 Montpellier Cedex 5, France
[3] Groupe d'Étude des Semiconducteurs, UMR CNRS 5650, Université Montpellier II, place Bataillon, 34095 Montpellier Cedex 5, France
[4] Departamento de Fisicà Aplicada, Universidad de Salamanca, Plaza Merced s/n 37008 Salamanca, Spain
E-mail: jf.millithaler@unile.it, lino.reggiani@unile.it, pousset@cem2.univ-montp2.fr, luca.varani@univ-montp2.fr, Christophe.Palermo@univ-montp2.fr, knap.wojciech@gmail.com, javierm@usal.es, tomasg@usal.es, susana@usal.es and dpardo@usal.es

Received 20 June 2008
Accepted 21 July 2008
Published 7 January 2009

Online at stacks.iop.org/JSTAT/2009/P01040
doi:10.1088/1742-5468/2009/01/P01040

Abstract. By means of numerical simulations we investigate the plasma frequency associated with voltage fluctuations in an n-type $In_{0.53}Ga_{0.47}As$ layer of thickness W and submicron length L embedded in a dielectric medium at $T = 300$ K. For $W = 100$ nm and carrier concentrations of 10^{16}–10^{18} cm^{-3} the results are in good agreement with the standard three-dimensional (3D) expression for the plasma frequency. For $W \leq 10$ nm the results exhibit a plasma frequency that depends on L, thus implying that the oscillation mode is dispersive. The corresponding frequency values are in good agreement with the two-dimensional (2D) expression for the plasma frequency obtained for a collisionless regime within the in-plane approximation for the self-consistent electric field. A region of crossover between the 2D and 3D behaviours of the plasma frequency, which we address as an open problem, is evidenced for

1742-5468/09/P01040+12$30.00

$W > 10$ nm. Problems associated with channel lengths shorter than the electron mean free path and the effects of an applied bias will be discussed.

Keywords: classical Monte Carlo simulations

Contents

1. Introduction

The spectral density of voltage fluctuations of a homogeneous macroscopic resistor at thermal equilibrium evidences a peak at the classical plasma frequency f_{p}, when the dielectric relaxation time ($\tau_{\mathrm{d}} = \rho\varepsilon_0\varepsilon_{\mathrm{mat}}$) is shorter than the plasma time, which for a three-dimensional (3D) geometry is given by

$$f_{\mathrm{p}}^{\mathrm{3D}} = \frac{1}{2\pi}\sqrt{\frac{e^2 n_0^{\mathrm{3D}}}{m_0 m \varepsilon_0 \varepsilon_{\mathrm{mat}}}} \tag{1}$$

with e the electron charge, n_0^{3D} the 3D average free carrier concentration and $\varepsilon_{\mathrm{mat}}$ the relative dielectric constant of the bulk material, ε_0 the vacuum permittivity, m_0 and m the free and effective electron masses, respectively. For a semiconductor material the plasma frequency can be controlled by means of an appropriate doping level in such a way as to be in the terahertz (THz) frequency range. Recently, one of the most promising strategies for obtaining THz radiation generation and detection by using electronic systems has been envisaged in exploiting the plasma approach. To this purpose, the scaling down of the dimensions to the nanometric size offers more possibility of modulating the value of the plasma frequency and of making use of nanodevices. In this framework, through an analytical approach, there was considered the case of a two-dimensional electron layer such as that constituted by the ungated channel of a nanometric transistor [1]. The electron gas was assumed as highly concentrated but non-degenerate, and supposed to undergo only long-range electron–electron interaction. By making a small signal analysis of the self-consistent set of drift, continuity and Poisson equations within the in-plane field approximation the electron gas is found to behave as the support of 2D standing waves

J. Stat. Mech. (2009) P01040

with frequency dispersion given by

$$f^{2D} = \frac{1}{2\pi}\sqrt{\frac{e^2 n_0^{2D} k}{2 m_0 m \varepsilon_0 \varepsilon_{diel}}} \tag{2}$$

where k is the in-plane wavevector, n_0^{2D} the average 2D carrier concentration and ε_{diel} the relative dielectric constant of the embedding medium. We notice that the 2D frequency depends on the relative dielectric constant of the external dielectric, thus coupling the source of the fluctuations, due to the free charge in the channel, with the external medium. Through the oscillations of the free charge, nanometric high electron mobility transistors have been suggested as possible emitters and detectors of electromagnetic radiation in the THz range [1, 2].

The aim of this work is to investigate the same system from a microscopic point of view, thus testing the limits of applicability of the analytical approach and improving the physical insight into the problem. To this purpose, we consider an n-type InGaAs layer embedded in a symmetric dielectric and investigate the plasma frequency characteristics by analysing the frequency spectrum of voltage fluctuations obtained from a Monte Carlo simulator coupled with a 2D Poisson solver. In the Ohmic regime, the spectrum of a 3D geometry is characterized by a peak at the plasma frequency associated with the carrier oscillations due to the self-consistent electric field [3], which is here called 'plasmonic noise'. Such a plasmonic peak is found to persist also in a 2D geometry [3]. However, the microscopic investigation of plasmonic voltage fluctuations in nanochannels evidences a complicate scenario [3], only partially in agreement with the simple 2D analytical approach of [1], and with several peculiarities which are proposed as open problems. Among them, the following three points are addressed below: (i) a region of crossover between the 2D and 3D behaviours of the plasma frequency, which is evidenced for channel width $W > 10$ nm and for channel length $L > 1$ μm; (ii) the role played by channel lengths shorter than the electron mean free path where transport enters a ballistic regime; (iii) the role played by the presence of an applied voltage sufficiently high for the current to be in the saturation regime.

The content of the work is organized as follows. Section 2 presents the theoretical approaches underlying the present investigation. Section 3 reports and discusses the numerical results obtained with a self-consistent Monte Carlo simulator. Major conclusions are summarized in section 4.

2. Monte Carlo simulations

The numerical solution of this problem is carried out by using a microscopic Monte Carlo approach coupled with a 2D Poisson solver as already detailed in [2, 4]. By evaluating the fluctuations of the voltage around the steady value in the centre of the device under test, the spectral density of this quantity is obtained from the corresponding correlation function, and the characteristic peaks exhibited by the spectrum before cut-off are analysed as detailed in [3]. To study the proper oscillations of the electron gas, we simulate a bar of $In_{0.53}Ga_{0.47}As$ of length L in the range 0.01–10 μm for different thicknesses W in the range 1–100 nm, carrier concentrations of 10^{16}–10^{18} cm^{-3}, with the two terminals of the bar connected by ideal Ohmic contacts. The contacts are realized by an infinite reservoir of thermalized electrons at electrochemical potentials differing by eU

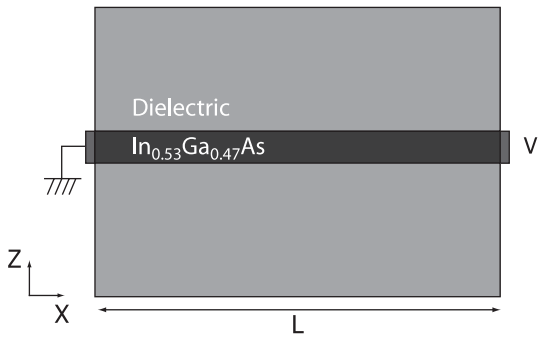

Figure 1. Schematic of the device (not to scale) studied within the Monte Carlo simulation. The free charge is present only in the bar of length L along the x direction and thickness W along the z direction. The terminal on the left-hand side is the source contact kept at a voltage $V = 0$; the terminal on the right-hand side is the drain contact kept at a potential V. Carriers are reflected at the boundaries between the bar and the dielectric.

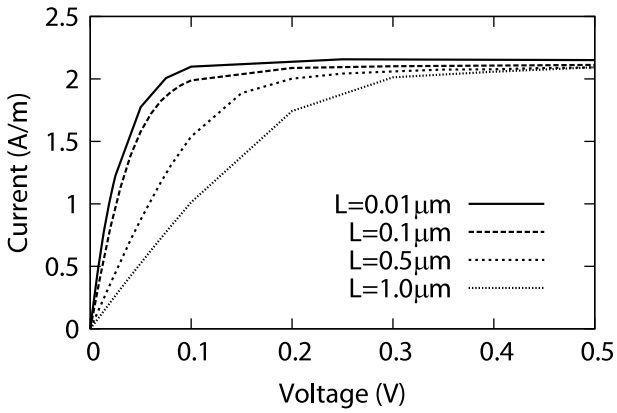

Figure 2. Current–voltage characteristics for a density of $n_0^{3D} = 10^{17}$ cm^{-3}, $W = 1$ nm and for different lengths. The current is given in A m^{-1} units because the third dimension does not enter the Poisson solver, and serves only to convert the number of simulated carriers into the 3D carrier concentration.

with U the applied voltage [5]. The bar is surrounded by a perfect dielectric (here taken as the vacuum) 10 μm wide in the upper and lower region of the bar, where the 2D Poisson equation in the xz-plane is solved to account for the fringing of the external electric field [6]. The third dimension is used to relate the number of simulated carriers with the 3D carrier concentration. For a comparative analysis between numerical simulations and analytical results of equation (2), we take $k = 2\pi/L$ and $n_0^{2D} = n_0^{3D}W$. The simulated structure, which is depicted in figure 1, represents a simplified version of an ungated transistor channel. The time and space discretizations take typical values of 0.2–1 fs for the time step, 0.1–5 nm for the spatial scale of the bar and 500 nm for the spatial scale of the dielectric. Typically there are about 80 carriers inside a mesh of the bar, which are found to provide a reliable solution of the Poisson equation. Table 1 reports the microscopic parameters of the material considered in calculations.

J. Stat. Mech. (2009) P01040

Table 1. Parameters of $In_{0.53}Ga_{0.47}As$.

Parameters	$In_{0.53}Ga_{0.47}As$		
Density (kg m^{-3})	5.545		
Sound velocity (m s^{-1})	4.756		
Static dielectric constant	13.88		
Optical dielectric constant	11.35		
LO phonon energy (eV)	0.0328		
Energy gap (eV)	0.7		
Alloy scattering potential (eV)	1.50		
	Γ	L	X
Effective mass (m^*/m_0)	0.042	0.258	0.538
Non-parabolicity (eV^{-1})	1.255	0.461	0.204
Energy level from Γ (eV)	0.0	0.61	1.11
Number of equivalent valleys	1	4	3
Acoustic deformation potential (eV)	5.887	10.84	9.657
Optical deformation potential (10^{10} eV m^{-1})	0.0	3.79	0.0
Optical phonon energy (eV)	0.0	0.0369	0.0
Intervalley deformation potential (10^{10} eV m^{-1})			
From Γ	0.0	7.827	11.32
From L	7.827	6.40	6.80
From X	11.32	6.80	8.537
Intervalley phonon energy (eV)			
From Γ	0.0	0.025 42	0.025 79
From L	0.025 42	0.248 1	0.030 21
From X	0.025 79	0.030 21	0.028 41

3. Results and discussion

Figure 2 reports the current–voltage characteristics for typical lengths in the range 0.01–1 μm and $n_0^{3D} = 10^{17}$ cm^{-3}. The curves exhibit a linear (Ohmic) regime at the lowest voltages and a saturation regime at the highest voltages, as expected for such a structure. For length $L \leq 0.1$ μm the transport enters the ballistic regime and the resistance is found to become independent of the length according to the ballistic expression [7]

$$R^{bal} = \frac{(2^3 k_B T m m_0)^{1/2}}{A\pi^{1/2} e^2 n_0^{3D}} \tag{3}$$

with A the cross-sectional area, k_B the Boltzmann constant, and T the bath temperature.

Figure 3 reports the velocity–field characteristics of the bulk material with the electric field taking values covering the range of the corresponding values of the voltage and length in figure 2. Here, the peak velocity, before the negative differential mobility region (NDM), is found to be 2.2×10^7 cm s^{-1} at the threshold field of 4.2 kV cm^{-1} for $n = 10^{17}$ cm^{-3} and 1.9×10^7 cm s^{-1} at the threshold field of 4.7 kV cm^{-1} for $n = 10^{18}$ cm^{-3}, respectively.

3.1. Ohmic regime

Figure 4 reports a typical spectrum of voltage fluctuations normalized to its zero-frequency value for the case of $L = 0.1$ μm, $W = 100$ nm, $n_0^{3D} = 10^{17}$ cm^{-3} in the absence of an

J. Stat. Mech. (2009) P01040

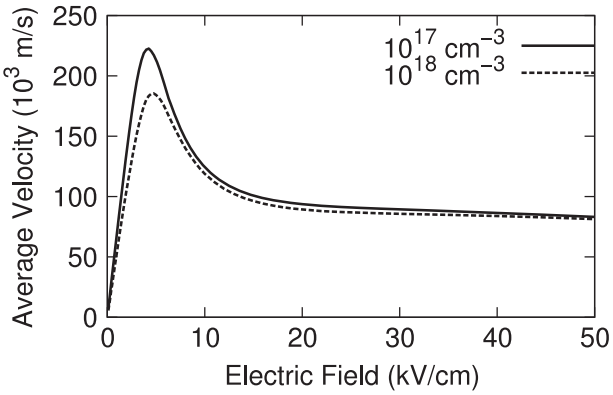

Figure 3. Velocity–field characteristic for a bulk $In_{0.53}Ga_{0.47}As$ with $n_0^{3D} = 10^{17}$ and 10^{18} cm^{-3}, at $T = 300$ K.

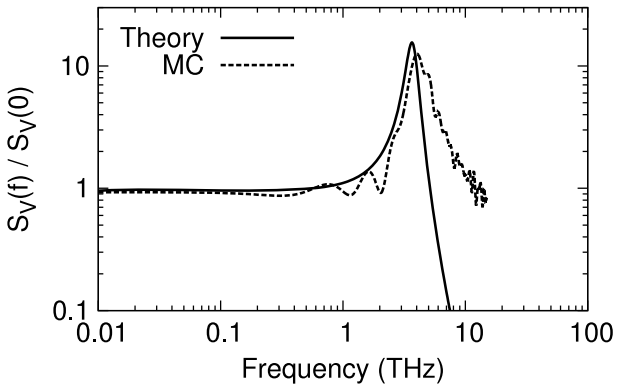

Figure 4. Spectral density of voltage fluctuations normalized to the static value in an $In_{0.53}Ga_{0.47}As$ channel of length $L = 0.1$ μm, width $W = 1$ nm at thermodynamic equilibrium. The dashed curve refers to simulations and the continuous curve to the theoretical expression for the equivalent circuit.

applied voltage. In this case we considered the right-hand contact of the channel in figure 1 as an open one. The results of the simulation (dotted curve) are compared with those obtained from the 3D impedance equivalent circuit (continuous curve) [8]:

$$\frac{S_V(f)}{S_V(0)} = \frac{1}{[1-(2\pi f\tau_P)^2]^2 + (2\pi f\tau_d)^2} \tag{4}$$

with f the signal frequency, $\tau_P = 4.28 \times 10^{-14}$ s, and $\tau_d = 1.07 \times 10^{-14}$ s the plasma and dielectric relaxation times corresponding to the simulated bulk material. Here, since $\tau_p > \tau_d$, the plasma peak is well evidenced, and is found to be in good agreement with the theoretical results of equation (4). We notice that simulations evidence a cut-off decay as f^{-2}, which is reminiscent of the presence of scattering mechanisms, instead of the sharper f^{-4} predicted by the equivalent circuit model. This point is investigated in figure 5, which reports a set of 3D spectra with increasing carrier concentrations. Here, the spike at the plasma frequency is fitted with a Gaussian $M \exp[-(f - f_P)^2/f_0^2]$ with M the amplitude and f_0 a dispersion frequency whose values are taken to better evidence the peak. The

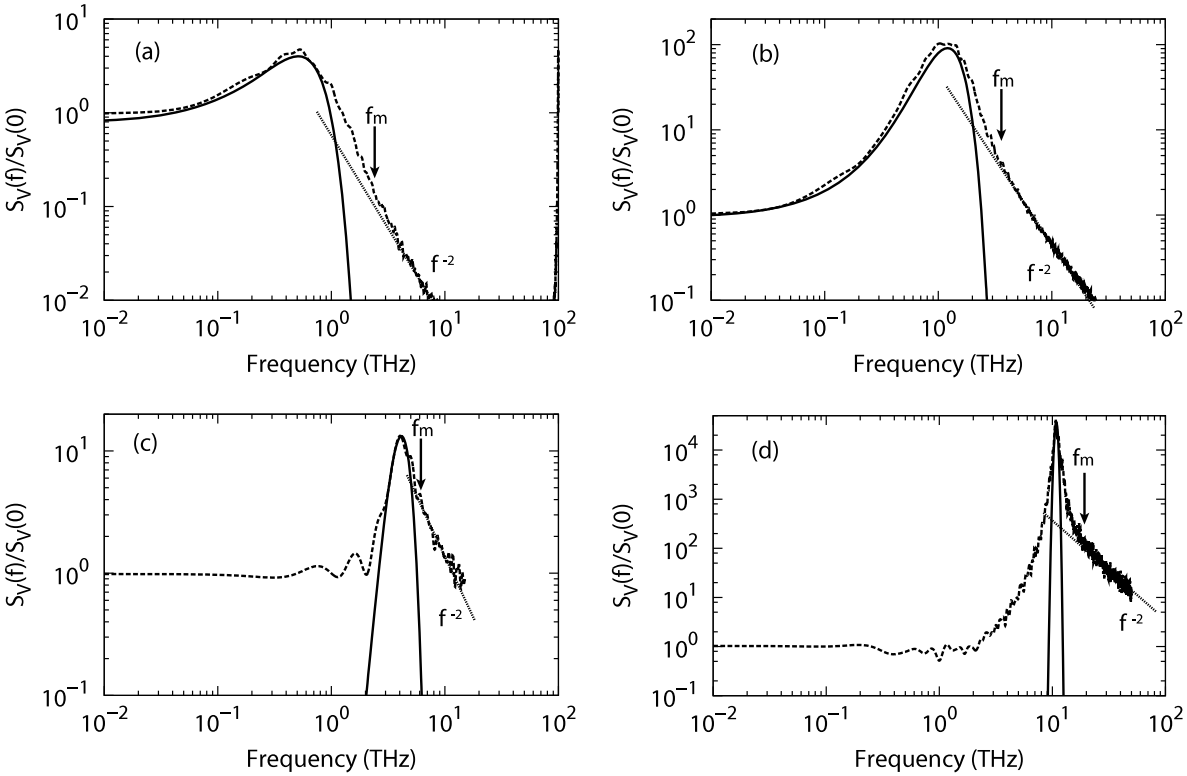

Figure 5. Spectra of voltage fluctuation normalized to the static value for the case of $W = 100$ nm and for electron densities $n_0^{3D} = 10^{15}$–10^{18} cm^{-3}. The continuous lines are the fitting curves with slope f^{-2} and f_m is the scattering rate obtained by interpolation.

asymptotic behaviour of the Lorentzian tail is found to intersect with the initial decay of the peak at frequency values f_m which is in good agreement with the momentum scattering rate, $1/\tau_m$ at the given carrier concentration.

Figure 6 reports the frequency of the peak exhibited by the spectral density of voltage fluctuations as a function of the channel length for different widths of the channel and a carrier concentration of 10^{17} cm^{-3}. Here, the numerical uncertainty is estimated to be within a factor of 2 at worst. For lengths below about 100 nm the transport enters the ballistic regime and the values of the frequency peak above the 3D plasma values might be attributed to the mixed action of 2D plasma oscillations and ballistic transport. In the diffusive regime we found: (i) for $W = 1$ and 2 nm we have found a reasonable agreement between the frequency peak of the simulations and those obtained from the 2D analytical formula in equation (2) over the whole range of lengths; (ii) for $W = 100$ nm, the frequency peak agrees well with the 3D analytical formula in equation (1) over the whole range of lengths; (iii) for $W = 5$ and 10 nm, a reasonable agreement of the frequency peak with the 2D analytical formula in equation (2) is limited to channel lengths in the 0.1–2 μm range, while, for some actually unsolved reasons, for L greater than 2 μm the frequency peak recovers the value of the 3D case, as for $W = 100$ nm.

The results for the 1 and 100 nm thicknesses represent asymptotic behaviours of 2D and 3D plasma and point to the existence of a crossover which is not predicted

J. Stat. Mech. (2009) P01040

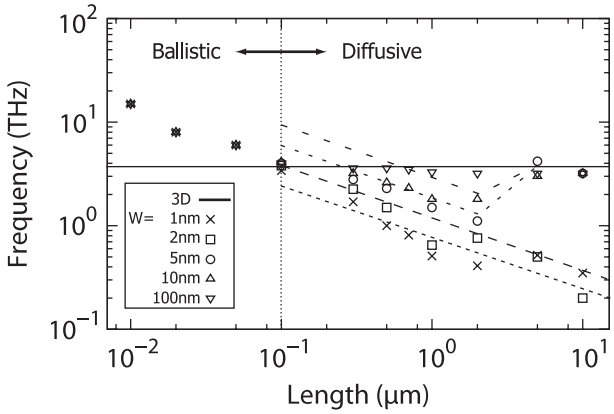

Figure 6. Plasma frequency as a function of the channel length $L = 10^{-2}$–10 μm for an electron density $n_0^{3D} = 10^{17}$ cm^{-3} and for different channel widths from 1 to 100 nm (cf inset). The continuous line refers to the 3D form of equation (1), the dashed lines with slope $1/\sqrt{L}$ serve as guides to the eyes.

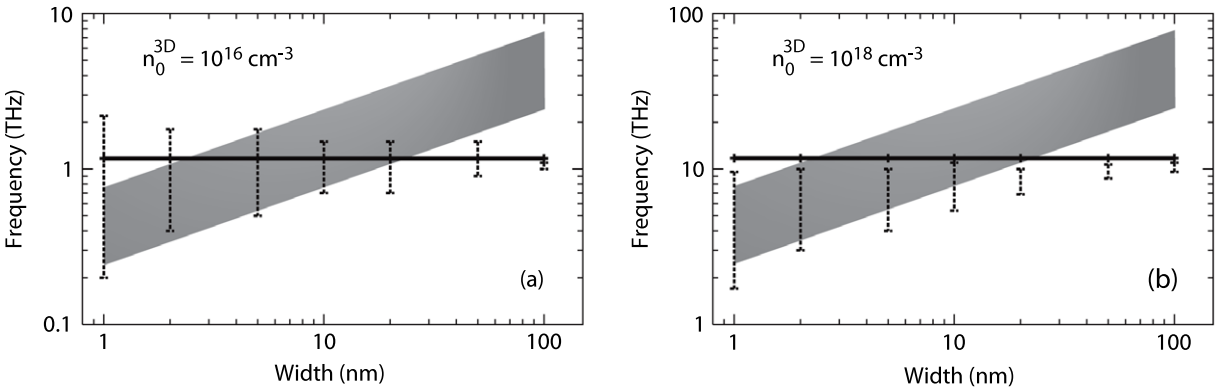

Figure 7. Plasma frequency as a function of the channel width for electron density $n_0^{3D} = 10^{16}$ cm^{-3} (a) and 10^{18} cm^{-3} (b). The continuous line refers to the 3D form of equation (1), the shaded region refers to the 2D form of equation (2) covering the two cases of $L = 0.1$ and 1 μm; the dashed bars refer to Monte Carlo results for the same two cases.

by the analytical theory. Accordingly, the crossover region has been investigated by simulating different thicknesses in the intermediate region $W = 10$–50 nm. The results are summarized in figure 7. Here the plasma frequencies obtained by simulations are reported together with the theoretical values of equations (1) and (2), for 3D carrier concentration of 10^{16} cm^{-3} (see figure 7(a)) and 10^{18} cm^{-3} (see figure 7(b)). We notice that the region of crossover is centred at about 10 nm, which compares well with the value of the 3D Debye length, $L_D = 14$ nm, for $n = 10^{16}$ cm^{-3}. Surprisingly, analogous results are obtained for the 3D carrier concentration of 10^{18} cm^{-3} reported in figure 7(b), where we would have expected a shift of the region of crossover at shorter width. The lack of a detailed theory for a 2D Debye screening together with this numerical result is addressed as an open problem.

J. Stat. Mech. (2009) P01040

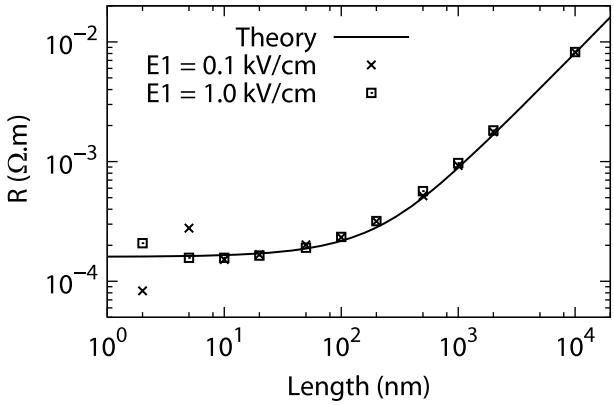

Figure 8. Ohmic resistance as function of the channel length showing the transition between ballistic and diffusive transport regimes.

We conclude that the simulations evidence the presence of a crossover between the 2D and 3D behaviours of the plasma frequency, not predicted by the analytical approach [1], which is controlled by the thickness and/or the length of the channel. The frequency peak covering different cases is in the 0.2–20 THz region.

3.2. Ballistic regime

Figure 8 reports the Ohmic resistance obtained by the V/I ratio of simulations at low voltages as a function of the channel length. The transition from a ballistic to diffusive regime is found to well agree with the analytical expression [9]

$$\frac{R}{R^{\mathrm{bal}}} = \Gamma(r) = 2r\{1 - r[1 - \exp(-r^{-1})]\} \tag{5}$$

with $r = \tau_m/\tau_T = 1.09\ l/L$ where τ_m is the collision time, $\tau_T = L/v_0$, with $v_0 = (8k_{\mathrm{B}}T/\pi m m_0)^{1/2}$ the oriented thermal velocity, the ballistic transit time, and $l = v_{\mathrm{th}}\tau_m$, with $v_0 = (2k_{\mathrm{B}}T/3mm_0)^{1/2}$ the random thermal velocity, the carrier mean free path.

Figure 9 reports the ballistic spectra for 10^{17} cm^{-3} and $L = 1$–100 nm. While for the smallest length we cannot clearly define a peculiar frequency apart from the value of the cut-off which is reminiscent of the ballistic transit time of the carrier, the samples with $L \geq 10$ nm exhibit a peak whose value increases as $1/\sqrt{L}$ in good agreement with the 2D theory. Nevertheless the fact that the peak is independent of W, as we can see in figure 6, is not explained.

3.3. Saturation regime

Figure 10 reports the spectral density of voltage fluctuations for $L = 0.5$ μm, left column, and $L = 1$ μm, right column, with $n_0^{3\mathrm{D}} = 10^{17}$ cm^{-3}, $W = 1$ nm, and at increasing voltages up to 2 V corresponding to velocity–field characteristics entering inside the NDM region. Here, the presence of NDM starts playing a dominant role at 0.5 V, see figure 10(b), where the plasma peak well evidenced at 0 V is replaced by a shoulder region in the range 0.1–2 THz, just before cut-off. Then, by further increasing the voltage at 1 V, see figure 10(c), we observe the onset of a frequency peak in the range of 0.1–0.2 THz, which is a

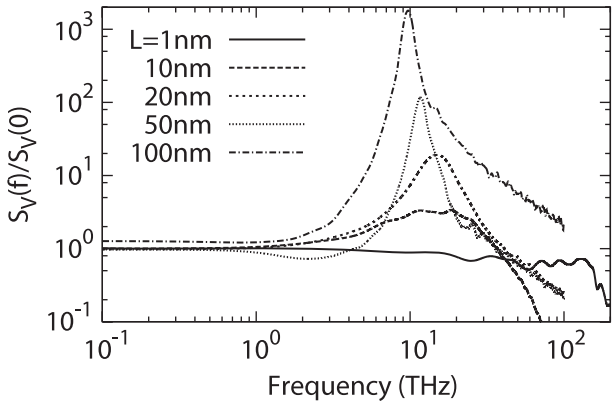

Figure 9. Spectra of voltage fluctuation normalized to the static value for an electron density $n_0^{3D} = 10^{18}$ cm^{-3}, a channel width $W = 1$ nm and for different channel lengths covering the ballistic region $L = 1$–10^2 nm.

precursor for the onset of current oscillations due to travelling Gunn domains [10]. Current oscillations have been observed in simulations at $U = 2$ V for channel lengths above about 1 μm (see figure 10(d) right column), where the Kroemer criterion [11] $n_0^{3D}L > 10^{11}$ cm^{-2} is satisfied. This interpretation is confirmed by the fact that the frequency peak shifts at lower frequencies on increasing the length of the channel with a $1/L$ behaviour as expected.

We conclude that by increasing the applied voltage to values inside the NDM region, the plasma peak is washed out in favour of the appearance of a new peak which is a precursor of the onset of current oscillations due to the establishment of the Gunn domains. For the channel lengths considered, the values of these Gunn oscillations are found to be in the range 0.1–0.5 THz.

4. Conclusions

Through a Monte Carlo calculation of the spectral density of voltage fluctuations we have investigated THz oscillations in $In_{0.53}Ga_{0.47}As$ channels embedded in an external dielectric as function of channel length and thickness, carrier concentration, and strength of the applied voltage. The microscopic investigation of the characteristic frequency peaks in voltage fluctuations of ultrathin InGaAs channels evidence a rich scenario, only partially predicted by the 2D collisionless analytical model [1].

Under near thermal equilibrium (Ohmic) conditions, the results of simulations show that for thick channels, i.e. W above 100 nm, 3D plasma oscillations appear independently of the channel length in the presence of diffusive transport regime. By contrast, for thin channels, i.e. W below 100 nm, we have observed the transition from 3D to 2D plasma modes where the plasma frequency decreases on increasing the length of the channel in good agreement with the analytical model [1]. The simulations show: (i) that the presence of scattering does not influence the value of the plasma frequency predicted by the collisionless theory and (ii) the existence of a crossover between the 2D and 3D behaviour of the plasma frequency, which happens at thicknesses above about 10 nm. In these conditions the plasmonic peak can take values in a wide range of frequencies from 0.2 to 10 THz according with different channel geometries, and carrier concentrations.

J. Stat. Mech. (2009) P01040

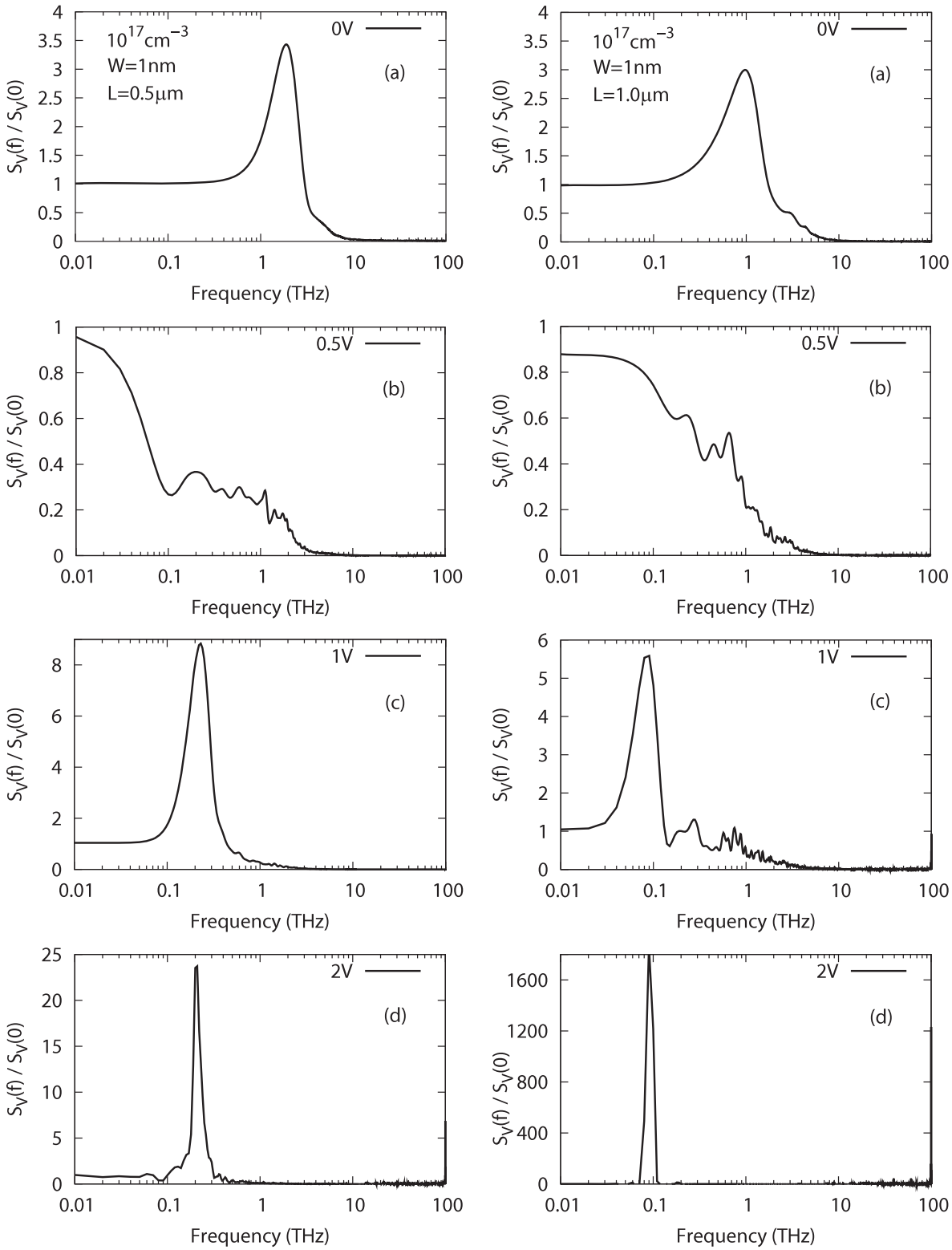

Figure 10. Spectrum of voltage fluctuations normalized to the static value for $L = 0.5$ and 1.0 μm (left and right columns, respectively), with $W = 1$ nm, $n_0^{3D} = 10^{17}$ cm^{-3}, and applied voltages in the range 0–2 V.

J. Stat. Mech. (2009) P01040

However, the frequency behaviour of structures with $W = 5$ and 10 nm exhibiting 2D and 3D behaviour depending of the length is at present an open problem.

Under the ballistic regime, achieved when $L \leq 100$ nm, the simulations exhibit a frequency peak which is unexpectedly independent of W, and whose amplitude decreases significantly on lowering their channel length.

Under saturation conditions, the results of simulations show: (i) the onset of a frequency peak, associated with the presence of NDM conditions, (ii) the onset of current oscillations, due to the transit of Gunn domains, and (iii) the washing out of the plasma peak. In this case the value of the frequency peak scales with the inverse of the channel length, taking values in a somewhat narrow frequency range 0.1–0.5 THz for channel lengths in the region 0.2–1 μm. Finally, we would like to stress that the electrostatic screening for a 2D electron gas remains in general an unsolved problem.

Acknowledgments

The work was supported by: CNRS-GDR and GDR-E projects 'Semiconductor sources and detectors of THz frequencies', the Region Languedoc-Roussillon-project 'Platforme Technologique THz', the Dirección General de Investigación (MEC, Spain), the FEDER through the project TEC2007-61259MIC and the Action integrada HF 2007-0014, the Italy–France bilateral project Galileo 2007–2008, the Spain–France bilateral project Picasso 2007–2008.

References

[1] Dyakonov M and Shur M S, 2005 *Appl. Phys. Lett.* **87** 111501
[2] Lusakowski J, Knap W, Dyakonova N, Varani L, Mateos J, González T, Roelens Y, Bollaert S, Cappy A and Karpierz K, 2005 *J. Appl. Phys.* **97** 064307
[3] Millithaler J-F, Reggiani L, Pousset J, Varani L, Palermo C, Knap W, Mateos J, González T, Perez S and Pardo D, 2008 *Appl. Phys. Lett.* **92** 042113
[4] Mateos J, González T, Pardo D, Hoël V and Cappy A, 2000 *IEEE Trans. Electron Devices* **47** 1950
[5] Bulashenko O M, Mateos J, Pardo D, González T, Reggiani L and Rubi J M, 1998 *Phys. Rev.* B **57** 1366
[6] Shur M and Ryzhii V, 2003 *Int. J. High Speed Electron. Syst.* **13** 575
[7] Greiner A, Reggiani L, Kuhn T and Varani L, 2000 *Semicond. Sci. Technol.* **15** 1071
[8] Varani L and Reggiani L, 1994 *Riv. Nuovo Cimento* **17** 1
[9] Butcher P, 1998 *Phys. Rev.* B **58** 9639
[10] Shiktorov P, Gruzhinskis V, Starikov E, Reggiani L and Varani L, 1996 *Phys. Rev.* B **54** 8821
[11] Kroemer H, 1964 *Proc. IEEE* **52** 1736

J. Stat. Mech. (2009) P01040